Available online at www.sciencedirect.com
SCIENCE DIRECT®
Measurement 36 (2004) 73–92
Measurement
www.elsevier.com/locate/measurement

Numerical double integration of acceleration measurements in noise

Y.K. Thong, M.S. Woolfson *, J.A. Crowe, B.R. Hayes-Gill, D.A. Jones

School of Electrical and Electronic Engineering, University of Nottingham, Nottingham NG7 2RD, United Kingdom

Received 31 July 2003; received in revised form 5 April 2004; accepted 9 April 2004

Abstract

In several applications one or more accelerometers are used to estimate position, which is derived by double integration of the acceleration measurements. An experimental method to calibrate the positional errors due to noise for an accelerometer has already been developed. In this paper, a theoretical formalism for this calibration method is derived, which is based on modelling the acceleration measurements as filtered noise. The effects of numerical integration are included in the model. Two accelerometers, with different noise ratings, are chosen for study. It is found that the theoretical model gives good quantitative agreement between theory and experiment for the variation of positional errors with integration time. The causes of the discrepancies between the theoretical and experimentally found results are discussed and suggestions are made for further research.

Keywords: Accelerometers; Microelectromechanical systems (MEMS); Inertial navigation systems (INS); Noise

1. Introduction

Accelerometers are used in many applications to determine position, sometimes in conjunction with other Inertial Navigation System (INS) devices, such as gyroscopes. Examples include devices used in pens and shoes [1] and measurement of forces and tilt on a vehicle under test [2], whilst Lee and Huang [3] describe a gyro-free all accelerometer INS.

Position is estimated from accelerometer measurements by a numerical double integration of the accelerometer signal. One concern when performing a numerical integration is that errors will occur because the numerical integration process is only approximating the underlying continuous signal to be integrated. Another factor to be taken into account is that the process of integrating noise leads to an output that has a root mean square value that increases with integration time, even in the absence of any motion of the accelerometer. The authors have been concerned with the latter problem.

The modelling of the noise in an accelerometer is by no means a straightforward problem. Djurić [4] has made a detailed study of the mechanisms of

* Corresponding author. Tel.: +44-115-951-5548; fax: +44-115-951-5616.
E-mail address: malcolm.woolfson@nottingham.ac.uk (M.S. Woolfson).

0263-2241/$ - see front matter © 2004 Elsevier Ltd. All rights reserved.
doi:10.1016/j.measurement.2004.04.005

noise sources in microelectromechanical systems (MEMS), concluding that the noise in an accelerometer can be modelled as coming from two sources: (i) thermal–mechanical noise and (ii) transistor noise, although it was also noted that more work is required for a full understanding. Pang and Liu [5] have looked at characterising the performance of a particular accelerometer when used in a robotic system. This work has looked particularly at the way of reducing the effect of the random thermal bias, which is modelled as integrated white noise, i.e. a random walk. Ball and Lewis [6] describe the various sources of noise affecting accelerometers where an estimate of the signal to noise ratio for the output displacement is made for an all-analogue system. Paez and Gibson [7] investigate possible chaotic behaviour in the estimated position for an accelerometer when it is subjected to sinusoidal and random inputs.

Some data sheets for accelerometers model noise as being filtered white noise and this is the general model that we will adopt in this paper. Discrepancies between theory and experiment will be due to neglect of other sources of corruption to the clean signal in the theory, for example due to temperature drift. The degree of comparison between theory and experiment will be a reflection of how important these other effects are.

Thong et al. [8] have made a detailed study into how the rms errors in estimated position for an accelerometer depend on integration time and also on the sampling frequency, f_s. An experimental method was devised to calibrate the accelerometer for errors in position due to noise and other effects. This method was also analysed theoretically, where the cases of dc bias, white and filtered noise were considered. In the theory, the rms error in the estimated position was determined by a direct analytical double integration of the acceleration measurements. Although this is an approximate model, the theoretical results for the variation of the rms error in position with time were in good agreement with experimental data taken from two commercially available accelerometers. However, this agreement could only be obtained by scaling the noise density given in the data sheets. The effects of numerical, rather than analytical, integration were not considered. It was also found that, for a fixed integration time, the rms errors in position were almost independent of sampling frequency when this frequency was larger than the Nyquist frequency.

The aim here is to extend the theory in [8] to include the effects of numerical, rather than analytical, integration into the double integration of accelerometer data. The differences between the results obtained with the rectangular and trapezoidal integration methods will be studied for the cases of general filtered noise, noise filtered with a single pole analogue filter and white noise.

The importance of the theoretical work is that expressions for the expected values of the rms errors in position due to noise could be compared with experimentally derived data to assess the relative significance of noise compared with drift effects. This information could be used to decide on whether drift effects should be compensated for in the real-time processing of the signals.

The importance of the experimental calibration procedure is that it can give a measurement of the expected maximum rms error in estimated position due to noise and other effects given a certain integration time. Alternatively, given a maximum acceptable error in position, then a maximum integration time can be specified before the accelerometer is reset.

2. Experimental estimation of accelerometer position errors [8]

In [8], a practical method is described to calibrate an accelerometer in terms of errors in estimated position as a function of time. Measurements are taken from a stationary, rather than a moving, accelerometer so as to separate out contributions to rms position errors from noise from those errors arising from the numerical integration of specific signals. The data set is divided up into M blocks of N samples and within each block of data, double integration is carried out using the trapezoidal rule. Taking the actual position as zero, the error in position at the Nth (i.e. last) sample in each block is computed and the mean square error is computed over all M blocks. The square root of the mean square error is taken

to obtain the root mean square (rms) error. This procedure is repeated for other block sizes and the rms error can then be obtained as a function of N or time; further details are contained in [8].

In [8], measurements were taken with the accelerometer at rest on an optical bench. In order to perform Monte-Carlo type estimations of the rms errors as a function of time, 30 min of data were recorded at a sampling frequency of 3 kHz, resulting in 5.4×10^6 samples of data.

Experimental data were taken from two different accelerometers: (1) Analog Devices ADXL202 [9] and (2) Crossbow CXL01LF3 [10]. The noise power spectral density is given by $1/2\sigma_c^2$ $\mathrm{cm^2\,s^{-4}\,Hz^{-1}}$. For the ADXL202, σ_c is rated at around 500 $\mu\mathrm{g\,Hz^{-0.5}}$ [9]. This value is significantly higher than the corresponding value for the CXL01LF3, which is 100 $\mu\mathrm{g\,Hz^{-0.5}}$ [10]. The 3 dB frequency for the low pass filter in-built to the Crossbow is set equal to 125 Hz; this value can be varied for the ADXL202 and values of 50, 200 and 500 Hz were used in the measurements.

The output of the Analogue to Digital Converter used has a nominal zero level of 2.5 V. However, it has been found, in practice, that the dc value is not exactly equal to 2.5 V and subtracting this value off the whole data segment could result in a bias that would significantly affect the doubly integrated results. To avoid this, the mean value over each block of N samples is computed and is subtracted off each sample within that block.

In Fig. 1, the experimental rms estimation errors in position are plotted for the ADXL and Crossbow accelerometers respectively. The 3 dB cut-off frequency of the ADXL is set at 50 Hz and the corresponding value for the Crossbow is fixed at 125 Hz. The sampling frequency used is 3 kHz in each case.

The curves show an increase in rms error in position with increasing integration time. If we plot this information on a log–log plot, Fig. 2, we can see that these plots are approximately straight lines. In the case of the ADXL, the slope of the log–log plot between integration times of 0.033 and 3.333 s is 1.596, whilst the corresponding value for the Crossbow is 1.926. This implies an approximate variation of the rms errors in estimated position, $\mathrm{RMS}(s(T))$ with integration time, T as

$$\mathrm{RMS}(s(T)) \propto T^{\alpha} \tag{1}$$

with $\alpha = 1.596$ and 1.926 for the ADXL and Crossbow respectively.

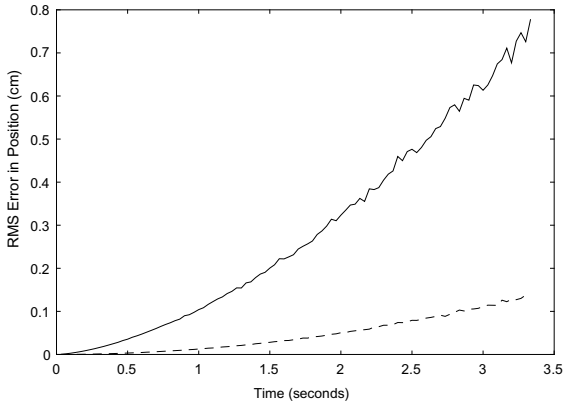

Fig. 1. Experimental RMS errors in position as a function of integration time. Full line: ADXL; dashed line: Crossbow.

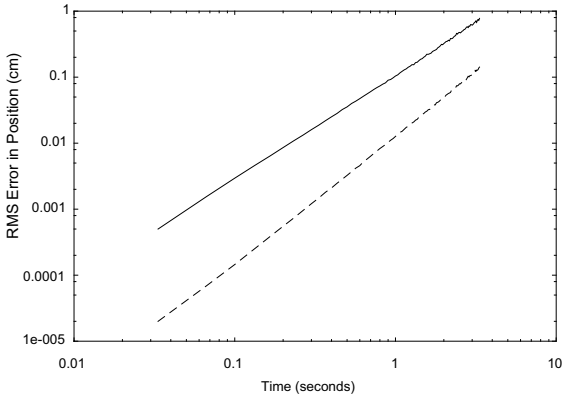

Fig. 2. Experimental RMS Errors in position as a function of integration time for accelerometers plotted on a log–log scale. Full line: ADXL; dashed line: Crossbow.

3. Review of analytical model, [8]

In this section, the analytical model derived in [8] will be briefly reviewed. In this model, the rms errors in the acceleration signal are considered

over each integration interval T and an *analytical* double integration is carried out to compute the rms errors in position. In particular *numerical* aspects of the double integration are not considered.

3.1. RMS error in double integration of white noise from a stationary accelerometer

Consider a data segment of T seconds duration of an accelerometer signal. Suppose that this segment is sampled with sampling frequency f_s Hz and N samples of the acceleration signal are processed so that $N = Tf_s$.

The following assumptions are made about the signal:

(1) The data are modelled as white noise with no "signal" component, i.e. an absolutely, stationary horizontal accelerometer.
(2) It is assumed that the data are stationary.

There are two effects contributing to the dependence of the rms errors in position on integration time. Firstly, as one integrates over more samples, that is N increasing, the rms value of the mean, or dc value, of the acceleration will decrease with time according to

$$\frac{\sigma_d}{\sqrt{N}} = \frac{\sigma_d}{\sqrt{Tf_s}} \tag{2}$$

where σ_d is the standard deviation of each noise sample. However, double integration of this rms value introduces a factor $\frac{1}{2}T^2$ to the rms errors in position.

Combining these two factors, the rms errors in position vary with integration time and sampling frequency according to the factor

$$\frac{\sigma_d}{\sqrt{Tf_s}} \cdot \frac{T^2}{2} = \frac{1}{2}\frac{\sigma_d T^{1.5}}{\sqrt{f_s}}. \tag{3}$$

This represents an overall increase of rms error in position with increasing integration time according to $T^{1.5}$.

A more detailed derivation of Eq. (3) can be found in [8].

3.2. Double integration of a bias

As a comparison, it is of interest to consider the rms errors in position, when the underlying acceleration signal is a bias A. In this case, the rms error in position is simply

$$\mathrm{RMS}(s(T)) = \frac{1}{2}AT^2 \tag{4}$$

that is, the rms error increases with integration time as T^2.

3.3. Double integration of filtered noise

The accelerometers under test have a built-in anti-aliasing filter. Hence, in practice one is double integrating coloured noise where there are correlations between different samples of the signal. In particular, Eq. (2), for the rms error in the acceleration measurements is no longer valid. In [8] a theoretical expression for the variation with integration time of the rms error in position for such filtered noise is derived.

4. Effects of numerical integration on errors in position

4.1. Comparison of analytical and numerical integration

In practice, one would be performing the double integration numerically. In order to illustrate the discrepancy between the analytical model and numerical integration, the rms errors in position as a function of time for white noise have been computed in two ways:

(1) Using the analytical model, Eq. (3).
(2) Using computer simulation. Here, a white Gaussian noise signal is generated on a computer and double integration is carried out using the rectangular rule. The following normalised parameters are used: discrete noise standard deviation, $\sigma_d = 1$, sampling frequency $f_s = 1$ Hz. 100 000 Monte-Carlo runs are used to calculate the mean square errors as a function of time. The square root of the mean square errors is taken to obtain the rms errors.

The results are shown in Fig. 3(a). It can be seen that the rms errors in position are underestimated by the theoretical expression, Eq. (3), which is shown as a dashed curve in the figure.

The log–log plots of both curves are shown in Fig. 3(b). The slopes (1.5) of the two curves are approximately the same except for the first few sample points of the computer simulated results, hence the variation of rms errors in position for white noise is correctly predicted to increase with integration time as $T^{1.5}$. The constant shift between the two curves in Fig. 3(b) suggests that the constant prefactor of 1/2 in the theoretical expression, Eq. (3) is inappropriate for numerical integration.

The estimated position at each time point is Gaussian distributed about the actual value. To see this, referring to the calculations in Fig. 3(a), we have plotted in Fig. 3(c) a histogram of the errors in position at the 100th data point for all 100 000 Monte-Carlo runs. Now the rms error at this data point is 573.1. Superimposed on top of this histogram is the Gaussian distribution function for a standard deviation of 573.1, taking into account the width of each bin in the histogram and the total number of samples. There is excellent agreement between the distribution function and the histogram, confirming that the position errors follow a Gaussian distribution.

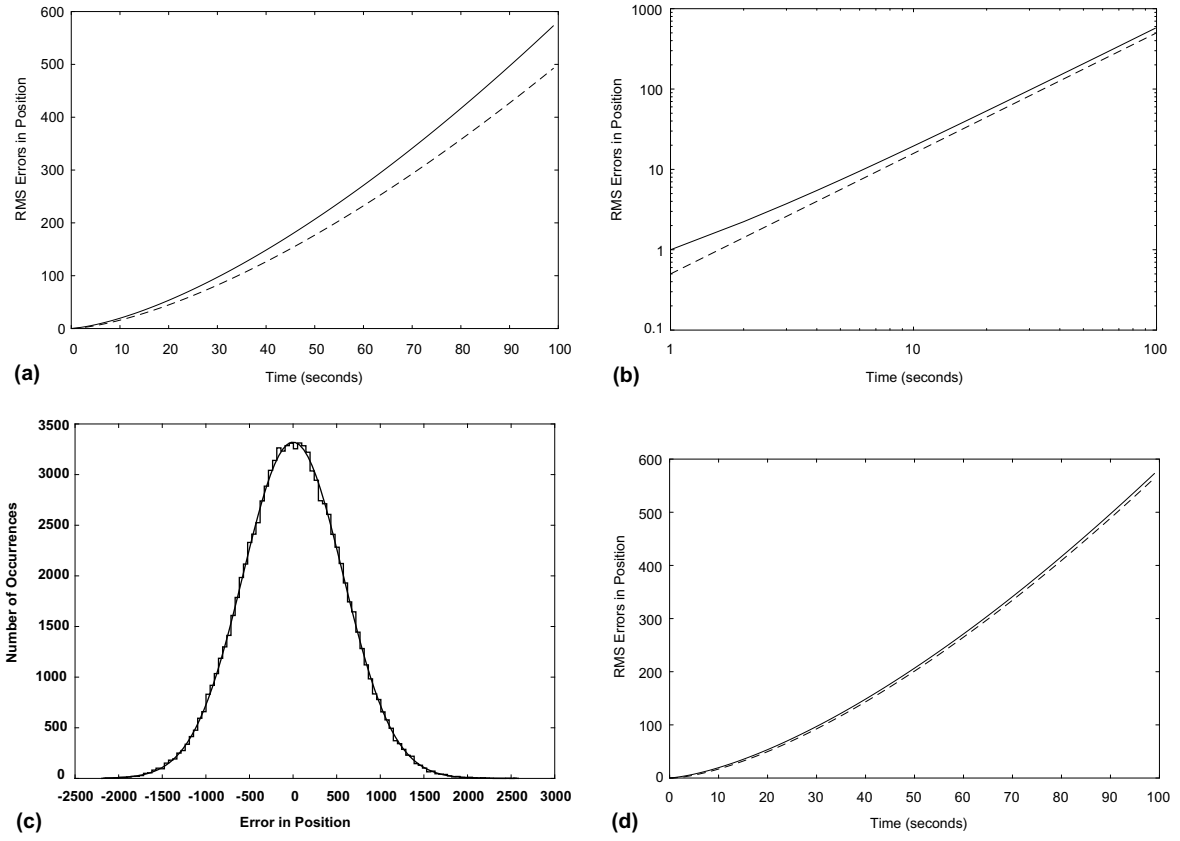

Fig. 3. Comparison of RMS errors in position versus integration time for white noise measurements. (a) Linear plot. Full curve: computer simulated errors; dashed curve: theory (Eq. (3). (b) Log–log plot. Full curve: computer simulated errors; dashed curve: theory (Eq. (3)). (c) Stepped curve. Histogram of errors in position at the 100th time point for the calculation in Fig. 3(a). Smooth curve: Gaussian distribution. (d) Comparison of computer simulated results in (a) with Eq. (22). Full curve: computer simulated errors; dashed curve: theory (Eq. (22)).

4.2. Numerical integration: rectangular and trapezoidal rules

Let $f(t)$ be the integrand of interest. Suppose that this signal is sampled with a sampling frequency of f_s. The numerical integral at the Nth sample evaluated using the rectangular rule is given by:

$$I_{\mathrm{RECT}}[N] = \Delta \sum_{n=2}^{N} f[n] \tag{5}$$

where $f[n]$ is the nth sample of $f(t)$, $\Delta = 1/f_s$ is the time between samples and the nth sample corresponding to the continuous time $t = (n-1)\Delta$. Note that it is assumed that $I_{\mathrm{RECT}}[1] = 0$; in this work the displacement will be related to a single integration involving the acceleration measurements (see Eq. (9) below) and hence this initial condition corresponds to a reference of zero displacement at $t = 0$.

The corresponding expression for the trapezoidal rule is given by

$$I_{\mathrm{TRAP}}[N] = \Delta \sum_{n=2}^{N-1} f[n] + \frac{\Delta}{2}(f[1] + f[N]) \tag{6}$$

Comparing Eq. (6) with Eq. (5) for $I_{\mathrm{RECT}}[N]$, it can be shown that

$$I_{\mathrm{TRAP}}[N] = I_{\mathrm{RECT}}[N] + \frac{\Delta}{2}(f[1] - f[N]) \tag{7}$$

4.3. Direct double integration of acceleration as a single integration

Formally, double integration of acceleration, $a(t)$, to obtain displacement, $s(t)$, can be written as

$$s(T) = \int_0^T \left[\int_0^t a(t')\,\mathrm{d}t' \right] \mathrm{d}t \tag{8}$$

where is assumed that the accelerometer is initially at rest with zero displacement.

This may be simplified to an expression involving a single integration (Appendix A):

$$s(T) = \int_0^T (T - t) \cdot a(t) \cdot \mathrm{d}t \tag{9}$$

Using Eq. (9), the numerical evaluation of $s(T)$ using the rectangular rule can be derived by writing $T = (N-1)\Delta$ and $t = (n-1)\Delta$, so that the integrand becomes

$$f[n] = ((N-1)\Delta - (n-1)\Delta)a[n] = (N-n)\Delta a[n] \tag{10}$$

Substituting for $f[n]$ from Eq. (10) into Eq. (5):

$$s_{\mathrm{RECT}}[N] = \Delta^2 \sum_{n=2}^{N} (N-n)a[n] \tag{11}$$

Using Eq. (7), the corresponding expression for the numerical evaluation of displacement using the trapezoidal rule is given by

$$s_{\mathrm{TRAP}}[N] = s_{\mathrm{RECT}}[N] + \frac{\Delta}{2}(f[1] - f[N]) \tag{12}$$

From Eq. (10):

$$f[1] = (N-1)\Delta a[1] \quad \text{and} \quad f[N] = 0 \tag{13}$$

Hence in Eq. (12):

$$s_{\mathrm{TRAP}}[N] = s_{\mathrm{RECT}}[N] + \frac{\Delta^2}{2}(N-1)a[1] \tag{14}$$

5. Errors in position determination

5.1. General result for filtered noise

5.1.1. Rectangular integration

In Appendix B.1, the expectation value of the square error in position is derived when rectangular integration is carried out, Eq. (11), on filtered noise. The result is as follows:

$$\begin{aligned} E\left[(s_{\mathrm{RECT}}[N])^2\right] = {} & \frac{r[0]}{6f_s^4}(N-1)(N-2)(2N-3) \\ & + \frac{1}{3f_s^4}\sum_{k=1}^{N-3} k^3 r[k] \\ & - \frac{1}{f_s^4}(N_1^2 + N_1 + 1/3)\sum_{k=1}^{N-3} kr[k] \\ & + \frac{1}{3f_s^4}N_1(2N_1^2 + 3N_1 + 1)\sum_{k=1}^{N-3} r[k] \end{aligned} \tag{15}$$

where $N_1 = N - 2$ and $r[k]$ is the kth lag of the autocorrelation function of the filtered noise.

The rms error in position at the Nth sample point is given by

$$\mathrm{RMS}[s_{\mathrm{RECT}}[N]] = \sqrt{E\left[(s_{\mathrm{RECT}}[N])^2\right]} \tag{16}$$

5.1.2. Trapezoidal integration

In Appendix B.2, the expectation value of the square error in position when trapezoidal integration (Eq. (14)) is carried out, is derived and the result is as follows:

$$\mathrm{RMS}[s_{\mathrm{TRAP}}[N]] = \sqrt{E\left[(s_{\mathrm{TRAP}}[N])^2\right]} \tag{17}$$

where

$$E\left[(s_{\mathrm{TRAP}}[N])^2\right] = E\left[(s_{\mathrm{RECT}}[N])^2\right] + \Delta^4(N-1) \times \left[(N-1)\sum_{n=1}^{N-2} r[n] - \sum_{n=1}^{N-2} n \cdot r[n]\right] + \frac{\Delta^4}{4}(N-1)^2 r[0] \tag{18}$$

5.2. White noise

For sampled white noise, the autocorrelation function at lag k in Eq. (15) becomes:

$$r[k] = \sigma_{\mathrm{d}}^2 . \delta_{k0} \tag{19}$$

where δ_{k0} is the Kronecker delta and σ_{d} is the standard deviation of the discrete noise.

Substituting for $r[k]$ from Eq. (19) into Eq. (15):

$$E\left[(s_{\mathrm{RECT}}[N])^2\right] = \frac{\sigma_{\mathrm{d}}^2}{6 f_{\mathrm{s}}^4}(N-1)(N-2)(2N-3) \tag{20}$$

Converting this expression to a function of time by substituting

$$N = T f_{\mathrm{s}} + 1 \tag{21}$$

it can be shown that

$$\mathrm{RMS}(s_{\mathrm{RECT}}(T)) = \frac{\sigma_{\mathrm{d}}}{\sqrt{6} f_{\mathrm{s}}^2}\left[(2Tf_{\mathrm{s}} - 1)(Tf_{\mathrm{s}} - 1)Tf_{\mathrm{s}}\right]^{0.5} \tag{22}$$

where T is the integration time, σ_{d} is the standard deviation of the acceleration noise and f_{s} is the sampling frequency. $\mathrm{RMS}(s_{\mathrm{RECT}}(T))$ in Eq. (22) is plotted as a function of time in Fig. 3(d). There is now seen to be excellent agreement between theory and computer simulations.

In particular, from Eq. (22), it should be noted that for large enough integration times, so that $T \gg \frac{1}{f_{\mathrm{s}}}$

$$\mathrm{RMS}(s_{\mathrm{RECT}}(T)) \approx \frac{1}{\sqrt{3}} \frac{\sigma_{\mathrm{d}}}{\sqrt{f_{\mathrm{s}}}} T^{1.5} \tag{23}$$

which differs from the theoretical expression in Eq. (3) by a factor of $2/\sqrt{3} = 1.155$. This result is also derived in Pollock [11], Farrell and Borth [12] although not from the perspective of using numerical integration.

It can be seen from Eqs. (18)–(20) that, for trapezoidal integration of white noise, the rms errors in the estimated position are given by:

$$\mathrm{RMS}((s_{\mathrm{TRAP}}(T))) = \sqrt{\frac{\sigma_{\mathrm{d}}^2}{6 f_{\mathrm{s}}^4} T f_{\mathrm{s}}(T f_{\mathrm{s}} - 1)(2T f_{\mathrm{s}} - 1) + \frac{\Delta^4}{4} T^2 f_{\mathrm{s}}^2 \sigma_{\mathrm{d}}^2} \tag{24}$$

Comparing with Eq. (22), it can be seen that for large enough T:

$$\mathrm{RMS}((s_{\mathrm{TRAP}}(T))) \approx \mathrm{RMS}((s_{\mathrm{RECT}}(T))) \tag{25}$$

This is verified in Fig. 4, where the theoretical positional errors when using the trapezoidal method are compared with those obtained with the rectangular method for the same conditions as for the simulation in Fig. 3. It can be seen that there is no noticeable difference between the rms errors from the two numerical integration techniques. Although not presented in this paper, there is also found to be excellent agreement between Eq. (24) and the corresponding computer simulated results, in that the two curves are indistinguishable when plotted on the same graph.

It should be noted that, in this case, using a higher order of integration does not lead to a reduction in noise in the estimated position. Hence, the choice of numerical integration method would be determined by the time dependence of the signal under study rather than on the noise.

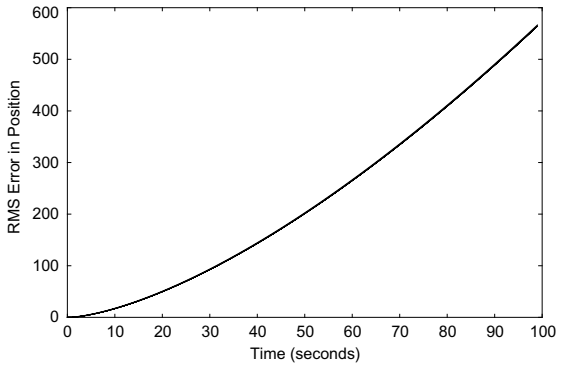

Fig. 4. Comparison of RMS errors in position versus integration time for white noise measurements: Comparison of results from rectangular and trapezoidal rules. Full curve: trapezoidal rule, Eq. (24); dashed curve: rectangular rule, Eq. (22).

5.3. Single pole model of anti-aliasing filter

In practice, the acceleration data is filtered by an in-built anti-aliasing filter, prior to being converted to digital form. For both the Crossbow and ADXL accelerometers, this filter is a single pole filter, where the autocorrelation function at lag k is given by

$$r[k] = A\exp(-\beta k) \tag{26}$$

where

$$A = \frac{\pi f_c \sigma_c^2}{2} \tag{27}$$

and

$$\beta = \frac{2\pi f_c}{f_s}. \tag{28}$$

The variance of the positional errors, Eq. (15), for rectangular integration then becomes:

$$\begin{aligned} E\left[(s_{\mathrm{RECT}}[N])^2\right] = {} & \frac{r[0]}{6f_s^4}(N-1)(N-2)(2N-3) \\ & + \frac{A}{3f_s^4}S_3(N-3) \\ & - \frac{A}{f_s^4}(N_1^2+N_1+1/3)S_1(N-3) \\ & + \frac{A}{3f_s^4}N_1(2N_1^2+3N_1+1)S_0(N-3) \end{aligned} \tag{29}$$

where

$$S_0(N) = \sum_{k=1}^{N}\exp(-\beta k) \tag{30}$$

$$S_1(N) = \sum_{k=1}^{N}k\exp(-\beta k) \tag{31}$$

and

$$S_3(N) = \sum_{k=1}^{N}k^3\exp(-\beta k) \tag{32}$$

The evaluations of these summations are given in Appendix C.

From Eq. (18), the corresponding result for trapezoidal integration becomes

$$\mathrm{RMS}(s_{\mathrm{TRAP}}[N]) = \sqrt{E\left[(s_{\mathrm{TRAP}}[N])^2\right]} \tag{33}$$

where

$$\begin{aligned} E\left[(s_{\mathrm{TRAP}}[N])^2\right] = {} & E\left[(s_{\mathrm{RECT}}[N])^2\right] + \Delta^4(N-1) \\ & \times A[(N-1)S_0(N-2) \\ & - S_1(N-2)] + \frac{\Delta^4}{4}(N-1)^2 r[0] \end{aligned} \tag{34}$$

and where $E[(s_{\mathrm{RECT}}[N])^2]$ is given by Eq. (29).

5.4. Impulse invariant digital filter

Eqs. (26)–(28) for $r[n]$ are applicable to the case where the accelerometer data is put through an anti-aliasing filter prior to digitisation; this model is appropriate for the analysis of experimental data. In Section 6.4, where the results of computer simulations will be presented, the expression is tested on samples of digitally filtered noise. We choose to use the impulse invariant method, where the impulse response of an analogue single pole filter is sampled directly to obtain the digital filter impulse response. This method leads to aliasing of the frequency response and should correspond more closely to the experimental situation than if the bilinear transform is used. The autocorrelation at lag k for the output from this type of digital filter is given by

$$r[k] = A\exp(-\beta k) \tag{35}$$

with

$$A = \frac{\beta^2\sigma_d^2}{1-\alpha^2} \tag{36}$$

where

$$\alpha = \exp\left(-\frac{2\pi f_c}{f_s}\right) \tag{37}$$

$$\beta = \frac{2\pi f_c}{f_s} \tag{38}$$

and σ_d^2 is the variance of the discrete noise.

The variance of the position errors for rectangular integration in this case is given by Eq. (29), with A and β given by Eqs. (36) and (38) respectively.

6. Errors in position determination with mean subtraction

6.1. General result for filtered noise

When performing the experimental calibration of the accelerometer (Section 2), it was found necessary to subtract off from each acceleration value in a given data segment, the mean value of the acceleration within that segment because of uncertainties in the dc level of the analogue to digital converter. This procedure is also appropriate in applications where the accelerometer comes to rest at the end of this trajectory as the velocity at time T is proportional to the mean value of the acceleration over that data interval.

Eq. (9) for the estimate of position, may be modified to take into account the subtraction of this mean from the data segment of duration T:

$$s(T) = \int_0^T (T-t)[a(t) - \bar{a}(T)]\cdot \mathrm{d}t \tag{39}$$

where the mean of the acceleration signal up to an integration time T is given by

$$\bar{a}(T) = \frac{1}{T}\int_0^T a(t)\cdot \mathrm{d}t \tag{40}$$

Separating Eq. (39) out into two terms:

$$s(T) = \int_0^T (T-t)\cdot a(t)\cdot \mathrm{d}t - \bar{a}(T)\cdot\int_0^T (T-t)\cdot \mathrm{d}t \tag{41}$$

Integrating the second term, putting in the limits and rearranging the terms:

$$s(T) = \frac{1}{2}\int_0^T (T-2t)\cdot a(t)\cdot \mathrm{d}t \tag{42}$$

Using Eq. (42), the numerical evaluation of $s(T)$ using the rectangular rule can be derived by writing $T = (N-1)\Delta$ and $t = (n-1)\Delta$, so that the integrand in Eq. (42) becomes

$$\begin{aligned} f[n] &= \frac{1}{2}((N-1)\Delta - 2(n-1)\Delta)a[n] \\ &= \frac{1}{2}(N-2n+1)\Delta a[n] \end{aligned} \tag{43}$$

Substituting for $f[n]$ from Eq. (43) into Eq. (5), the following relation between displacement and acceleration is obtained for rectangular integration:

$$s_{\mathrm{RECT}}^{\mathrm{SUB}}[N] = \frac{\Delta^2}{2}\sum_{n=2}^{N}(N-2n+1)a[n] \tag{44}$$

where the superscript "SUB" indicates that the mean of the data over N samples has been subtracted.

The corresponding result can be obtained for trapezoidal integration by noting that from Eq. (43):

$$f[1] = \frac{\Delta}{2}(N-1)a[1] \quad \text{and}$$

$$f[N] = -\frac{\Delta}{2}(N-1)a[N]$$

Hence in Eq. (7):

$$\begin{aligned} s_{\mathrm{TRAP}}^{\mathrm{SUB}}[N] = s_{\mathrm{RECT}}^{\mathrm{SUB}}[N] &+ \frac{\Delta^2}{4}(N-1)a[1] \\ &+ \frac{\Delta^2}{4}(N-1)a[N] \end{aligned} \tag{45}$$

6.1.1. Rectangular integration

In Appendix D.1, the expectation value of the square error in position when rectangular

integration is carried out on filtered noise, is derived and the result is as follows:

$$E\left[\left(s_{\mathrm{RECT}}^{\mathrm{SUB}}[N]\right)^2\right] = \frac{r[0]}{12f_s^4}(N-1)(N^2-2N+3) + \frac{1}{3f_s^4}\sum_{k=1}^{N-2}k^3 r[k] - \frac{1}{6f_s^4}(3N^2-6N+5) \times \sum_{k=1}^{N-2}kr[k] + \frac{1}{6f_s^4}(N-1) \times (N^2-2N+3)\sum_{k=1}^{N-2}r[k] \quad (46)$$

The rms error in position at the Nth sample point is thus given by

$$\mathrm{RMS}\left[s_{\mathrm{RECT}}^{\mathrm{SUB}}[N]\right] = \sqrt{E\left[\left(s_{\mathrm{RECT}}^{\mathrm{SUB}}[N]\right)^2\right]} \quad (47)$$

6.1.2. Trapezoidal integration

In Appendix D.2 the expectation value of the square error in position when trapezoidal integration is carried out is derived and the result is as follows.

$$E\left[\left(s_{\mathrm{TRAP}}^{\mathrm{SUB}}[N]\right)^2\right] = E\left[\left(s_{\mathrm{RECT}}^{\mathrm{SUB}}[N]\right)^2\right] - \frac{\Delta^4}{8}(N-1)^2 \times r[N-1] - \frac{\Delta^4}{8}(N-1)^2 r[0] \quad (48)$$

and hence the rms error is given by

$$\mathrm{RMS}\left[s_{\mathrm{TRAP}}^{\mathrm{SUB}}[N]\right] = \sqrt{E\left[\left(s_{\mathrm{TRAP}}^{\mathrm{SUB}}[N]\right)^2\right]} \quad (49)$$

6.2. White noise

Substituting for $r[k]$ from Eq. (19) into Eq. (46), we find the variance for the error in position for white noise at the Nth sample point as

$$E\left[\left(s_{\mathrm{RECT}}^{\mathrm{SUB}}[N]\right)^2\right] = \frac{\sigma_d^2}{12f_s^4}(N-1)(N^2-2N+3) \quad (50)$$

Converting this expression to a function of time using Eq. (21), it can be shown that

$$\mathrm{RMS}\left(\left(s_{\mathrm{RECT}}^{\mathrm{SUB}}[N]\right)\right) = \sqrt{E\left[\left(s_{\mathrm{RECT}}^{\mathrm{SUB}}[N]\right)^2\right]} = \sqrt{\frac{\sigma_d^2}{12}\frac{Tf_s\left(T^2f_s^2+2\right)}{f_s^4}} \quad (51)$$

For integration times $T \gg 1/f_s$, the following approximation can be made:

$$\mathrm{RMS}\left(s_{\mathrm{RECT}}^{\mathrm{SUB}}(T)\right) \approx \frac{\sigma_d}{2\sqrt{3}}\cdot\frac{T^{1.5}}{\sqrt{f_s}} \quad (52)$$

Comparing Eq. (52) with (23), we see that the effect of the subtraction of the mean on the rms position errors is to halve them. The same large-time approximation can be derived for trapezoidal integration.

Eq. (51) is verified in Fig. 5, where a comparison is made between the computer simulated and theoretical rms errors as a function of integration time when subtracting the mean and using the rectangular rule. The signal and noise parameters are the same as were used in the simulations presented in Fig. 3. There is seen to be excellent agreement between the theoretical calculation and computer simulation results.

From Eqs. (19), (48) and (49), the rms error when double integrating white noise when using the trapezoidal rule is given by

$$\mathrm{RMS}\left(s_{\mathrm{TRAP}}^{\mathrm{SUB}}[N]\right) = \sqrt{E\left[\left(s_{\mathrm{TRAP}}^{\mathrm{SUB}}[N]\right)^2\right]} \quad (53)$$

where

$$E\left[\left(s_{\mathrm{TRAP}}^{\mathrm{SUB}}[N]\right)^2\right] = E\left[\left(s_{\mathrm{RECT}}^{\mathrm{SUB}}[N]\right)^2\right] - \frac{\Delta^4}{8}(N-1)^2\sigma_d^2 \quad (54)$$

For large N, the rms positional error when double integrating white noise using the trapezoidal rule can be shown to be given by Eq. (50), the same result as when the rectangular rule is used.

6.3. Single pole model for anti-aliasing filter

Substituting for $r[k]$ from Eq. (26) into Eq. (46), the variance of the positional error for rectangular integration at the Nth sample point becomes:

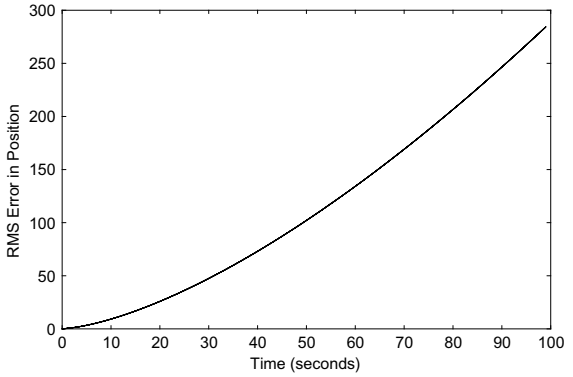

Fig. 5. Comparison of RMS errors in position versus integration time for white noise measurements, rectangular rule, with subtraction of mean. Full curve: computer simulated errors; dashed curve: theory (Eq. (51)).

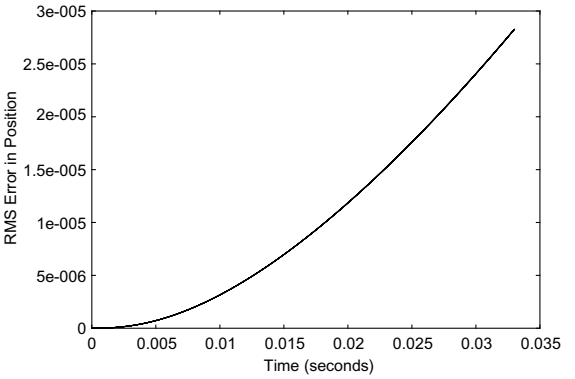

Fig. 6. Comparison of RMS errors in position versus integration time for filtered noise measurements, trapezoidal rule. Full curve: computer simulated errors; dashed curve: theory (Eqs. (56) and (57)).

$$E\left[\left(s^{\mathrm{SUB}}_{\mathrm{RECT}}[N]\right)^2\right] = \frac{r[0]}{12f_s^4}(N-1)(N^2-2N+3) + \frac{A}{3f_s^4}S_3(N-2) - \frac{A}{6f_s^4}(3N^2-6N+5)S_1(N-2) + \frac{A}{6f_s^4}(N-1)(N^2-2N+3) \times S_0(N-2) \quad (55)$$

where the summations $S_0(N)$, $S_1(N)$ and $S_3(N)$ are given in Appendix C.

From Eqs. (26) and (48), the corresponding result for trapezoidal integration becomes

$$\mathrm{RMS}\left(s^{\mathrm{SUB}}_{\mathrm{TRAP}}[N]\right) = \sqrt{E\left[\left(s^{\mathrm{SUB}}_{\mathrm{TRAP}}[N]\right)^2\right]} \quad (56)$$

$$E\left[\left(s^{\mathrm{SUB}}_{\mathrm{TRAP}}[N]\right)^2\right] = E\left[\left(s^{\mathrm{SUB}}_{\mathrm{RECT}}[N]\right)^2\right] - \frac{\Delta^4}{8}(N-1)^2 \times A\exp(-\beta(N-1)) - \frac{\Delta^4}{8}(N-1)^2 A \quad (57)$$

6.4. Impulse invariant digital filter

For the impulse invariant filter, the rms error in displacement, when using the trapezoidal rule of integration, is given by Eqs. (56) and (57), where A and β are given by Eqs. (36) and (38).

In Fig. 6, the theoretical rms estimated errors are compared with the corresponding computer simulated values for the case where the impulse invariant low-pass digital filter is applied with a 3 dB cut-off of 50 Hz, $\sigma_d = 1$ and $f_s = 3$ kHz. The filter is run for 200 samples before integration begins to reduce the effects of the transients. Trapezoidal integration with subtraction of the mean is carried out. Rms errors are computed over 100 000 Monte-Carlo runs. It can be seen that there is excellent agreement between theory and computer simulated results.

7. Analysis of experimental data

The validity of Eqs. (56) and (57) is now tested by analysis of experimental data taken from the same two accelerometers described in Section 2 and studied by Thong et al. [8]. In this reference, σ_c was scaled so that agreement was obtained at an integration time of 3 s. This was necessary because the model used in [8] did not include the effects of numerical integration and mean subtraction. In this study, no such scaling takes place and the unscaled values for this parameter, as provided by the manufacturer's data sheets, are used: $\sigma_c = 0.491\ \mathrm{cm\,s^{-2}\,Hz^{-0.5}}$ for the ADXL [9] and $0.0981\ \mathrm{cm\,s^{-2}\,Hz^{-0.5}}$ for the Crossbow [10].

7.1. ADXL

In Fig. 7, the experimental variation of the rms errors in position as a function of integration time for sampling frequency of 3000 Hz is shown as a dashed line.

The theoretical curve calculated according to Eqs. (56) and (57) is shown on the same Figure as a full line. Eqs. (26)–(28) are used for $\{r[n]\}$ as in this case, analogue filtering takes place prior to sampling.

It can be seen that there is excellent agreement between theory and experiment for integration times up to about 1 s; thereafter the theory underestimates the positional error, with a discrepancy of 22% at an integration time of 3.333 s. The level of agreement is similar to that obtained in [8] except that in the work described in this paper, no scaling of σ_c is needed to obtain this agreement. In [8], σ_c needed to be scaled to 68% of the value given in the data sheets in order to obtain this level of agreement with the analytical model.

It is to be expected that the theory, Eqs. (56) and (57), should give a lower bound on the rms error in the estimate of position. This is because the model used in the derivation of this equation was that the acceleration measurements are realisations of filtered white noise. Drift effects, such as from temperature, have not been taken into account and these will tend to increase the position errors above that for filtered noise. At small integration times, low frequency drift effects will tend to be filtered off by the subtraction process, Eq. (39), as the drift will be approximately dc for small time segments. However, for larger data segments, variations in the drift will become more apparent and the simple mean subtraction will reduce, but not eliminate the drift. Hence, for larger integration times, experimental rms errors in position will tend to increase beyond the theoretical values predicted by Eqs. (56) and (57).

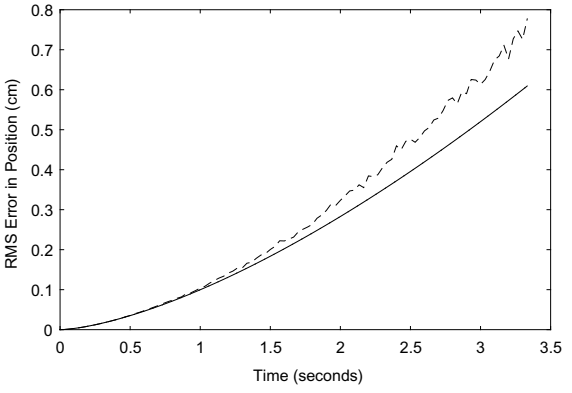

Fig. 7. RMS errors in position as a function of integration time for ADXL. Full curve: theory (Eqs. (56) and (57)); dashed curve: experimental data.

7.2. Crossbow

The corresponding comparison between theory, Eqs. (56) and (57), and experiment for the Crossbow accelerometer is shown in Fig. 8(a).

It can be seen that there is good quantitative agreement between theory and experiment with the discrepancy being 14% at an integration time of 3.333 s. However, there is seen to be a difference between how the errors vary with integration time, which can be seen clearly in Fig. 8(b) where the log of the rms positional error is plotted against log of integration time. The slope of the theoretical plot calculated between integration times of 0.0333 and 3.333 s is 1.513, whilst that of the experimental plot is 1.926. Hence, experimentally, the rms errors increase with time according to the bias model, Section 3.2, whilst the filtered noise model has been used in the theory. As for the ADXL, the unscaled value for σ_c is used in Eq. (27), which was not the case when the analytical model derived in [8] was used, where σ_c had to be reduced to 61% of the value given in the data sheets.

Now the Crossbow has a lower noise rating than the ADXL. Thong [13] has estimated the ratio of the peak-to-peak drift amplitude versus rms noise for these two accelerometers. For the ADXL, an approximate value for this ratio was found to be 0.38, whilst for the Crossbow this ratio was estimated as 2.85. Hence, drift is more significant for the Crossbow accelerometer. Thus, Eq. (57), which neglects drift, is expected to give worse agreement with experiment than for the ADXL, which is seen to be the case. The effects of drift will become more significant for larger integration times and it is clear from Fig. 8(a) that the

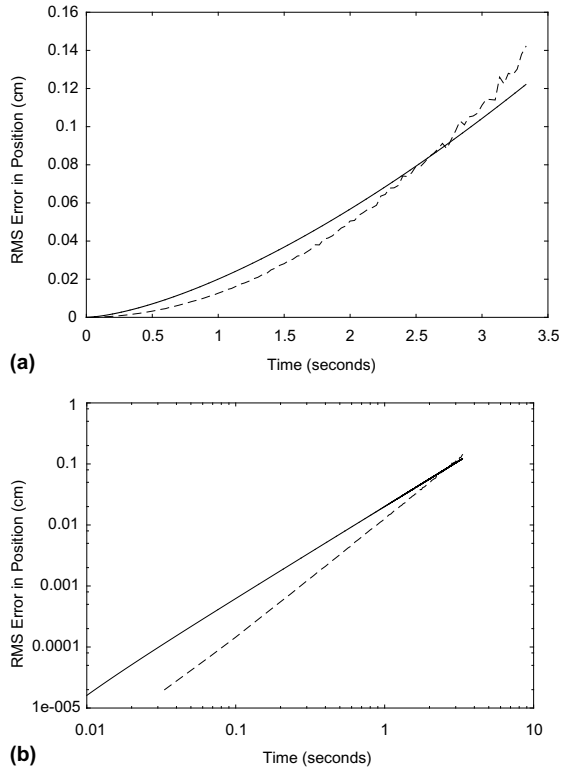

Fig. 8. RMS errors in position as a function of integration time for Crossbow. Full curve: theory (Eqs. (56) and (57)); dashed curve: experimental data. (a) Linear plot and (b) Log–log plot.

discrepancy between the theory predicted by Eq. (57) and experiment increases for integration time greater than about 2.8 s.

8. Conclusions

In this paper, the work of Ref. [8] has been extended to take into account the effects of numerical integration and subtraction of the mean when calibrating the positional errors for an accelerometer. Theoretical expressions for the rms positional error as a function of integration time have been derived taking into account numerical integration and subtraction of the mean from the acceleration measurements. There is now good agreement between theory and experiment (Figs. 7 and 8) without having to scale σ_c, which was required in Ref. [8].

One of the main contributions of this work and that of Ref. [8] is to present a practical method to calibrate the positional errors determined by double integration of accelerometer data. Data are taken for a stationary accelerometer, so that the calibration is taking into account thermal noise, drift and any other noise effects. This procedure separates out the errors due to the double integration of such effects from errors arising from the numerical double integration of specific signals. This latter problem could, for example, be evaluated by numerical integration of computer simulated signals that are appropriate for the particular application of interest. The separation of the contributions to the rms errors in position from double integration of the signal and double integration of noise and other effects provides useful information. For example, if the main errors come from double integration of the underlying clean signal, then one could consider increasing the sampling rate or using a different integration method. However, if it was found that the main errors come from the double integration of the noise and drift, then one could consider whether further filtering of the data is required prior to double integration, taking into account the bandwidth of the underlying clean signal.

We have considered in the paper two of the most basic integration methods, the rectangular rule and the trapezoidal rule. It would be of interest to investigate the effects on the errors in position when double integrating noise, using other numerical methods to perform the double integration. One example is Simpson's rule, which is often more accurate in double integration of signals. However, this does not mean that Simpson's rule would be necessarily be more robust to noise when applied to the double integration of noisy data. We have seen in this paper that the trapezoidal and rectangular rules yield very similar results in spite of the fact that the former is usually more accurate when integrating clean signals.

The discrepancies between theory and experiment are as informative as the agreements. For example, in Fig. 7, the excellent agreement between the theory and experiment up to an integration time of 1 s implies that noise effects are dominant over drift effects when double integrating

the acceleration signal. However, drift effects become more significant as the integration time is increased beyond this value and it may then be necessary to compensate for these drift effects, [5,14,15]. Hence, the theoretical results, Eqs. (56) and (57) give a lower bound on the positional errors in the absence of drift effects.

The discrepancy between theory and experiment for the variation of positional errors with time for the Crossbow accelerometer implies that the effect of drift is more significant than for the ADXL. Depending on the application, drift effects may need to be compensated for all integration times, [5,14,15]. Qualitatively we could see the significance of drift effects directly from the acceleration data for each type of accelerometer, but the calibration technique described here tells us over what ranges of integration times that this drift is significant.

One possible further line of research would be to incorporate the effects of drift into the analysis of positional errors, but this would require an assumption of the variation of the drift with time as well as its amplitude.

Acknowledgements

We would like to thank the referee for giving suggestions on how to improve the presentation of the paper.

Appendix A. Alternative expression for double integration

The displacement is given by direct double integration of the acceleration measurements:

$$s(T) = \int_0^T \left[\int_0^t a(t')\,\mathrm{d}t' \right] \mathrm{d}t \tag{A.1.1}$$

It should be noted that Eq. (A.1.1) is only valid for an accelerometer that is initially at rest at zero displacement, but this is the case for many applications.

This can be integrated by parts with

$$u = \int_0^t a(t') \cdot \mathrm{d}t', \quad \frac{\mathrm{d}u}{\mathrm{d}t} = a(t) \tag{A.1.2}$$

$\mathrm{d}v = 1$ and hence $v = t$.

Integrating by parts:

$$\begin{aligned} s(T) &= \left[t \int_0^t a(t') \cdot \mathrm{d}t' \right]_0^T - \int_0^T t \cdot a(t) \cdot \mathrm{d}t \\ &= T \int_0^T a(t') \cdot \mathrm{d}t' - \int_0^T t \cdot a(t) \cdot \mathrm{d}t \end{aligned} \tag{A.1.3}$$

which may be simplified to an expression involving a single integration:

$$s(T) = \int_0^T (T - t) \cdot a(t) \cdot \mathrm{d}t \tag{A.1.4}$$

Appendix B. RMS errors in position from numerical integration

B.1. Rectangular rule

The estimated displacement using the rectangular rule is given, from Eq. (11), by

$$s_{\mathrm{RECT}}[N] = \Delta^2 \sum_{n=2}^{N} (N - n) a[n] \tag{B.1.1}$$

Taking the square of both sides:

$$(s_{\mathrm{RECT}}[N])^2 = \Delta^4 \sum_{n=2}^{N} (N - n) a[n] \cdot \sum_{m=2}^{N} (N - m) a[m] \tag{B.1.2}$$

Taking expectation values of both sides:

$$\begin{aligned} E\left[(s_{\mathrm{RECT}}[N])^2 \right] = \Delta^4 \sum_{n=2}^{N} \sum_{m=2}^{N} &(N - n) \\ &\times (N - m) E[a[n] \cdot a[m]] \end{aligned} \tag{B.1.3}$$

Next, one can separate out this expression into a "self" term, Q_{SELF}, when $m = n$ and a "cross" term, Q_{CROSS}, when $m \neq n$:

$$Q_{\mathrm{SELF}} = \Delta^4 \sum_{n=2}^{N} (N - n)^2 E[(a[n])^2] \tag{B.1.4}$$

and

$$Q_{\mathrm{CROSS}} = \Delta^4 \sum_{n=2}^{N} \sum_{m=2}^{N} (N-n)(N-m) E[a[n] \cdot a[m]] \quad (n \neq m) \tag{B.1.5}$$

Assuming a stationary signal, one can write the autocorrelation function at lag $|n-m|$ as

$$r[|n-m|] = E[a[n] \cdot a[m]] \tag{B.1.6}$$

B.1.1. Evaluation of Q_{SELF}

Using Eq. (B.1.6), we can write

$$E[(a[n])^2] = r[0] \tag{B.1.7}$$

where $r[0]$ is the autocorrelation function at zero lag, or variance, for the acceleration measurements $\{a[n]\}$. Hence, we can write for Q_{SELF}:

$$Q_{\mathrm{SELF}} = \Delta^4 r[0] \sum_{n=2}^{N} (N-n)^2 \tag{B.1.8}$$

Expanding out the term in the summation:

$$Q_{\mathrm{SELF}} = \Delta^4 r[0] \left\{ N^2 \sum_{n=2}^{N} 1 - 2N \sum_{n=2}^{N} n + \sum_{n=2}^{N} n^2 \right\} \tag{B.1.9}$$

One can evaluate each of the summations on the right hand side as follows:

$$\sum_{n=2}^{N} 1 = (N-1) \tag{B.1.10}$$

$$\sum_{n=2}^{N} n = \sum_{n=1}^{N} n - 1 = \frac{N(N+1)}{2} - 1 = \frac{N^2+N-2}{2} \tag{B.1.11}$$

$$\sum_{n=2}^{N} n^2 = \sum_{n=1}^{N} n^2 - 1 = \frac{1}{6} N(N+1)(2N+1) - 1 \tag{B.1.12}$$

Substituting for these three summations into Eq. (B.1.9):

$$Q_{\mathrm{SELF}} = \Delta^4 r[0] \left\{ \frac{1}{6} N(N+1)(2N+1) - 1 \right\} - 2\Delta^4 r[0] N \frac{(N^2+N-2)}{2} + \Delta^4 r[0](N-1)N^2 \tag{B.1.13}$$

Collecting together these terms:

$$Q_{\mathrm{SELF}} = r[0]\Delta^4 \left\{ \frac{N^3}{3} - \frac{3N^2}{2} + \frac{13N}{6} - 1 \right\} \tag{B.1.14}$$

Factorising this expression and writing $\Delta = 1/f_s$ the following expression for Q_{SELF} is derived:

$$Q_{\mathrm{SELF}} = \frac{r[0]}{6 f_s^4} (N-1)(N-2)(2N-3) \tag{B.1.15}$$

B.1.2. Evaluation of Q_{CROSS}

Eq. (B.1.5) can be expanded out, using the relation

$$E[a[m] \cdot a[n]] = E[a[n] \cdot a[m]] = r[|m-n|] \tag{B.1.16}$$

as follows

$$Q_{\mathrm{CROSS}} = \sum_{k=1}^{N-3} Q_{\mathrm{CROSS}}^k \tag{B.1.17}$$

where

$$Q_{\mathrm{CROSS}}^k = \frac{2}{f_s^4} \left\{ \sum_{p=0}^{N-k-3} (N-2-p)(N-2-p-k) \right\} r[k] \tag{B.1.18}$$

Expanding this expression:

$$Q_{\mathrm{CROSS}}^k = \frac{2}{f_s^4} r[k](N-2)(N-2-k) \sum_{p=0}^{N-k-3} 1 + \frac{2}{f_s^4} r[k](4-2N+k) \sum_{p=0}^{N-k-3} p + \frac{2}{f_s^4} r[k] \sum_{p=0}^{N-k-3} p^2 \tag{B.1.19}$$

The summations may be evaluated as follows:

$$\sum_{p=0}^{N-k-3} 1 = N-k-2$$

$$\sum_{p=0}^{N-k-3} p = \frac{1}{2}(N-k-3)(N-k-2)$$

$$\sum_{p=0}^{N-k-3} p^2 = \frac{1}{6}(N-k-3)(N-k-2)(2N-2k-5) \tag{B.1.20}$$

Substituting for these summations into Eq. (B.1.19) and re-arranging terms, it can be shown that

$$\begin{aligned} Q^k_{\mathrm{CROSS}} = {} & \frac{2r[k]}{f_s^4}\left\{(N-2)^2 - 2(N-2)k + k^2\right\}(N-2) \\ & + \frac{r[k]}{f_s^4}\{(N-2)-1-k))((N-2)-k)\} \\ & \times \{k-2(N-2)\} + \frac{r[k]}{3f_s^4}\{((N-2)-k-1) \\ & \times ((N-2)-k)\}\{2(N-2)-2k-1\} \end{aligned} \tag{B.1.21}$$

Let $N_1 = N-2$ and collect together terms with identical powers of k:

$$\begin{aligned} Q^k_{\mathrm{CROSS}} = {} & \frac{r[k]}{f_s^4}\left\{\frac{k^3}{3} - k[N_1^2 + N_1 + 1/3]\right. \\ & \left. + \frac{N_1}{3}\left[2N_1^2 + 3N_1 + 1\right]\right\} \end{aligned} \tag{B.1.22}$$

B.1.3. Evaluation of $E\left[(s_{RECT}[N])^2\right]$

Now, from Eqs. (B.1.3) and (B.1.1):

$$E\left[(s_{\mathrm{RECT}}[N])^2\right] = Q_{\mathrm{SELF}} + \sum_{k=1}^{N-3} Q^k_{\mathrm{CROSS}} \tag{B.1.23}$$

Substituting for Q_{SELF} from Eq. (B.1.15) and Q^k_{CROSS} from Eq. (B.1.22) into Eq. (B.1.23), it can be shown that:

$$\begin{aligned} E\left[(s_{\mathrm{RECT}}[N])^2\right] = {} & \frac{r[0]}{6f_s^4}(N-1)(N-2)(2N-3) \\ & + \frac{1}{3f_s^4}\sum_{k=1}^{N-3} k^3 r[k] - \frac{1}{f_s^4}(N_1^2 \\ & + N_1 + 1/3)\sum_{k=1}^{N-3} kr[k] \\ & + \frac{1}{3f_s^4}N_1(2N_1^2 + 3N_1 + 1)\sum_{k=1}^{N-3} r[k] \end{aligned} \tag{B.1.24}$$

where $N_1 = N-2$.

B.2. Trapezoidal rule

From Eq. (14), the estimate in position using the trapezoidal rule is related to the corresponding estimate from the rectangular rule by

$$s_{\mathrm{TRAP}}[N] = s_{\mathrm{RECT}}[N] + \frac{\Delta^2}{2}(N-1)a[1] \tag{B.1.25}$$

where, from Eq. (11):

$$s_{\mathrm{RECT}}[N] = \Delta^2 \sum_{n=2}^{N}(N-n)a[n] \tag{B.1.26}$$

Taking the square of both sides of Eq. (B.1.25) and taking expectation values:

$$\begin{aligned} E\left[(s_{\mathrm{TRAP}}[N])^2\right] = {} & E\left[(s_{\mathrm{RECT}}[N])^2\right] \\ & + \Delta^2(N-1)E[a[1]\cdot s_{\mathrm{RECT}}[N]] \\ & + \frac{\Delta^4}{4}(N-1)^2 r[0] \end{aligned} \tag{B.1.27}$$

The first term on the right hand side is given in Eq. (B.1.24). To evaluate the second term, multiply both sides of Eq. (11) by $a[1]$ and take expectation values:

$$E[s_{\mathrm{RECT}}[N]\cdot a[1]] = \Delta^2 \sum_{n=2}^{N}(N-n)E[a[n]\cdot a[1]] \tag{B.1.28}$$

The Nth term in the summation is zero, hence using Eq. (B.1.16):

$$E[s_{\mathrm{RECT}}[N]\cdot a[1]] = \Delta^2 N\sum_{n=2}^{N-1} r[n-1] - \Delta^2\sum_{n=2}^{N-1} n\cdot r[n-1] \quad \text{(B.1.29)}$$

which can be rewritten as

$$E[s_{\mathrm{RECT}}[N]\cdot a[1]] = \Delta^2 N\sum_{n=1}^{N-2} r[n] - \Delta^2\sum_{n=1}^{N-2}(n+1)r[n] = \Delta^2(N-1)\sum_{n=1}^{N-2} r[n] - \Delta^2\sum_{n=1}^{N-2} nr[n] \quad \text{(B.1.30)}$$

$E[s_{\mathrm{RECT}}[N]\cdot a[1]]$, given in Eq. (B.1.30), is now substituted into Eq. (B.1.27) to obtain the final result, Eq. (18).

Appendix C. Evaluation of the summations

Define the following summations:

$$S_0(\beta;N) = \sum_{n=1}^{N} \exp(-\beta n) \quad \text{(C.1.1)}$$

$$S_1(\beta,N) = \sum_{n=1}^{N} n\cdot\exp(-\beta n) \quad \text{(C.1.2)}$$

$$S_3(\beta,N) = \sum_{n=1}^{N} n^3\cdot\exp(-\beta n) \quad \text{(C.1.3)}$$

For notational convenience, the dependence of S_0, S_1 and S_3 on β will not be made explicit.

Now

$$S_1(N) = -\frac{\partial S_0(N)}{\partial\beta} \quad \text{(C.1.4)}$$

and

$$S_3(N) = -\frac{\partial^3 S_0(N)}{\partial\beta^3} \quad \text{(C.1.5)}$$

$S_0(N)$ in Eq. (C.1.1) may be evaluated directly as

$$S_0(N) = \frac{\exp(-\beta)\cdot(1-\exp(-\beta N))}{1-\exp(-\beta)} \quad \text{(C.1.6)}$$

From Eq. (C.1.4):

$$S_1(N) = \frac{\exp(-\beta) - \exp(-\beta(1+N)) - N\exp(-\beta(1+N)) + N\exp(-\beta(2+N))}{(\exp(-\beta)-1)^2} \quad \text{(C.1.7)}$$

and from Eq. (C.1.5):

$$S_3(N) = \frac{f}{g} \quad \text{(C.1.8)}$$

where

$$\begin{aligned} f = {} & \exp(-\beta) + \exp(-3\beta) - 3N^2\exp(-\beta(1+N)) \\ & + 6N^2\exp(-\beta(N+2)) - \exp(-\beta(N+3)) \\ & - 3N^2\exp(-\beta(3+N)) + 3N^3\exp(-\beta(2+N)) \\ & - 3N^3\exp(-\beta(3+N)) + 3N\exp(-\beta(3+N)) \\ & + N^3\exp(-\beta(4+N)) - \exp(-\beta(1+N)) \\ & - N^3\exp(-\beta(1+N)) - 3N\exp(-\beta(1+N)) \\ & + 4\exp(-2\beta) - 4\exp(-\beta(2+N)) \end{aligned} \quad \text{(C.1.9)}$$

and

$$g = (\exp(-\beta)-1)^4 \quad \text{(C.1.10)}$$

Appendix D. RMS errors with subtraction of mean

D.1. Rectangular rule

The estimated displacement, with subtraction of the mean, using the rectangular rule is given, from Eq. (44), by

$$s^{\mathrm{SUB}}_{\mathrm{RECT}}[N] = \frac{\Delta^2}{2}\sum_{n=2}^{N}(N-2n+1)a[n] \quad \text{(D.1.1)}$$

Taking the square of both sides and then taking expectation values:

$$E\left[\left(s_{\mathrm{RECT}}^{\mathrm{SUB}}[N]\right)^2\right] = \frac{\Delta^4}{4}\sum_{n=2}^{N}\sum_{m=2}^{N}(N-2n+1) \times (N-2m+1)E[a[n]\cdot a[m]] \tag{D.1.2}$$

Next, one can separate out this expression into a "self" term, Q_{SELF}, when $m = n$ and a "cross" term, Q_{CROSS}, when $m \neq n$:

$$Q_{\mathrm{SELF}} = \frac{\Delta^4}{4}\sum_{n=2}^{N}(N-2n+1)^2E[(a[n])^2] \tag{D.1.3}$$

and

$$Q_{\mathrm{CROSS}} = \frac{\Delta^4}{4}\sum_{n=2}^{N}\sum_{m=2}^{N}(N-2n+1) \times (N-2m+1)E[a[n]\cdot a[m]] \quad (n \neq m) \tag{D.1.4}$$

D.1.1. Evaluation of Q_{SELF}

Using Eq. (B.1.7), we can write for Q_{SELF}:

$$Q_{\mathrm{SELF}} = \frac{\Delta^4}{4}r[0]\sum_{n=2}^{N}(N-2n+1)^2 \tag{D.1.5}$$

Expanding out the term in the summation, using the following identities:

$$\sum_{n=2}^{N}1 = (N-1) \tag{D.1.6}$$

$$\sum_{n=2}^{N}n = \sum_{n=1}^{N}n - 1 = \frac{N(N+1)}{2} - 1 = \frac{N^2+N-2}{2} \tag{D.1.7}$$

$$\sum_{n=2}^{N}n^2 = \sum_{n=1}^{N}n^2 - 1 = \frac{1}{6}N(N+1)(2N+1) - 1 \tag{D.1.8}$$

and rearranging terms, it can be shown that

$$Q_{\mathrm{SELF}} = \frac{r[0]\Delta^4}{12}\{(N-1)(N^2-2N+3)\} \tag{D.1.9}$$

D.1.2. Evaluation of Q_{CROSS}

Using the result (B.1.16), Eq. (D.1.4) can be written as:

$$Q_{\mathrm{CROSS}} = \sum_{k=1}^{N-2}Q_{\mathrm{CROSS}}^{k} \tag{D.1.10}$$

where

$$Q_{\mathrm{CROSS}}^{k} = \frac{1}{2f_s^4}\left\{\sum_{p=0}^{N-k-2}(N-3-2p)(N-3-2p-2k)\right\}r[k] \tag{D.1.11}$$

Expanding this expression and using the following identities:

$$\sum_{p=0}^{N-k-2}1 = N-k-1$$

$$\sum_{p=0}^{N-k-2}p = \frac{1}{2}(N-k-2)(N-k-1)$$

$$\sum_{p=0}^{N-k-2}p^2 = \frac{1}{6}(N-k-2)(N-k-1)(2N-2k-3) \tag{D.1.12}$$

and, rearranging terms, it can be shown that

$$Q_{\mathrm{CROSS}}^{k} = \frac{r[k]}{f_s^4}\left\{\frac{k^3}{3} - \frac{k}{6}[3N^2-6N+5] + \frac{(N-1)}{6}[N^2-2N+3]\right\} \tag{D.1.13}$$

D.1.3. Evaluation of $E\left[\left(s_{RECT}[N]\right)^2\right]$

Now, from Eqs. (D.1.2) and (D.1.4):

$$E\left[\left(s_{\mathrm{RECT}}^{\mathrm{SUB}}[N]\right)^2\right] = Q_{\mathrm{SELF}} + \sum_{k=1}^{N-2}Q_{\mathrm{CROSS}}^{k} \tag{D.1.14}$$

Substituting for Q_{SELF} from Eq. (D.1.9) and Q_{CROSS}^{k} from Eq. (D.1.11) into Eq. (D.1.14), it can be shown that:

$$E\left[\left(s_{\mathrm{RECT}}^{\mathrm{SUB}}[N]\right)^2\right] = \frac{r[0]}{12f_s^4}(N-1)(N^2-2N+3) + \frac{1}{3f_s^4}\sum_{k=1}^{N-2}k^3 r[k] - \frac{1}{6f_s^4}(3N^2-6N+5)\sum_{k=1}^{N-2}kr[k] + \frac{1}{6f_s^4}(N-1)(N^2-2N+3)\sum_{k=1}^{N-2}r[k] \quad \text{(D.1.15)}$$

D.2. Trapezoidal rule

From Eq. (45), the estimate in position using the trapezoidal rule is related to the corresponding estimate from the rectangular rule

$$s_{\mathrm{TRAP}}^{\mathrm{SUB}}[N] = s_{\mathrm{RECT}}^{\mathrm{SUB}}[N] + \frac{\Delta^2}{4}(N-1)a[1] + \frac{\Delta^2}{4}(N-1)a[N] \quad \text{(D.1.16)}$$

Taking the square of both sides of Eq. (D.1.16) and taking expectation values:

$$E\left[\left(s_{\mathrm{TRAP}}^{\mathrm{SUB}}[N]\right)^2\right] = E\left[\left(s_{\mathrm{RECT}}^{\mathrm{SUB}}[N]\right)^2\right] + \frac{\Delta^2}{2}(N-1) \times E\left[a[1]\cdot s_{\mathrm{RECT}}^{\mathrm{SUB}}[N]\right] + \frac{\Delta^2}{2}(N-1)E\left[a[N]\cdot s_{\mathrm{RECT}}^{\mathrm{SUB}}[N]\right] + \frac{\Delta^4}{16}(N-1)^2 r[0] + \frac{\Delta^4}{8}(N-1)^2 \times r[N-1] + \frac{\Delta^4}{16}(N-1)^2 r[0] \quad \text{(D.1.17)}$$

where $r[n]$ is defined in Eq. (B.1.16).

The first term on the right hand side is given in Eq. (D.1.15). To evaluate the second term, multiply both sides of Eq. (D.1.1) by $a[1]$ and take expectation values:

$$E\left[s_{\mathrm{RECT}}^{\mathrm{SUB}}[N]\cdot a[1]\right] = \frac{\Delta^2}{2}\sum_{n=2}^{N}(N-2n+1)E[a[n]\cdot a[1]] = \frac{(N+1)\Delta^2}{2}\sum_{n=2}^{N}r[n-1] - \Delta^2\sum_{n=2}^{N}n\cdot r[n-1] = \frac{(N+1)\Delta^2}{2}\sum_{p=1}^{N-1}r[p] - \Delta^2\sum_{p=1}^{N-1}(p+1)\cdot r[p] = \frac{(N-1)\Delta^2}{2}\sum_{p=1}^{N-1}r[p] - \Delta^2\sum_{p=1}^{N-1}p\cdot r[p] \quad \text{(D.1.18)}$$

To evaluate the third term on the right hand side of Eq. (D.1.17), multiply both sides of Eq. (D.1.1) by $a[N]$ and take expectation values:

$$E\left[s_{\mathrm{RECT}}^{\mathrm{SUB}}[N]\cdot a[N]\right] = \frac{\Delta^2}{2}\sum_{n=2}^{N}(N-2n+1)E[a[n]\cdot a[N]] = \frac{(N+1)\Delta^2}{2}\sum_{n=2}^{N}r[N-n] - \Delta^2\sum_{n=2}^{N}n\cdot r[N-n] \quad \text{(D.1.19)}$$

The right-hand side of this equation can be rewritten as follows:

$$E\left[s_{\mathrm{RECT}}^{\mathrm{SUB}}[N]\cdot a[N]\right] = \frac{(N+1)\Delta^2}{2}\sum_{p=0}^{N-2}r[p] - \Delta^2\sum_{p=0}^{N-2}(N-p)\cdot r[p] = \frac{(1-N)\Delta^2}{2}\sum_{p=0}^{N-2}r[p] + \Delta^2\sum_{p=1}^{N-2}p\cdot r[p] \quad \text{(D.1.20)}$$

Substituting for $E\left[s_{\mathrm{RECT}}^{\mathrm{SUB}}[N]\cdot a[1]\right]$ from Eq. (D.1.18) and $E\left[s_{\mathrm{RECT}}^{\mathrm{SUB}}[N]\cdot a[N]\right]$ from Eq. (D.1.19)

into Eq. (D.1.20) and combining terms, it can be shown that

$$E\left[\left(s^{\mathrm{SUB}}_{\mathrm{TRAP}}[N]\right)^2\right] = E\left[\left(s^{\mathrm{SUB}}_{\mathrm{RECT}}[N]\right)^2\right] - \frac{\Delta^4}{8} \times (N-1)^2 r[N-1] - \frac{\Delta^4}{8}(N-1)^2 r[0] \qquad \text{(D.1.21)}$$

References

[1] C. Verplaetse, Inertial proprioceptive devices: self-motion-sensing toys and tools, IBM Systems Journal 35 (3&4) (1996) 639–650.

[2] W. Stockwell, Measuring a vehicle's dynamic motion, Test and Measurement World 19 (3) (1999) 37–40.

[3] S.-C. Lee, Y.-C. Huang, Innovative estimation method with measurement likelihood for all-accelerometer type inertial navigation systems, IEEE Transactions on Aerospace and Electronic Systems 38 (2) (2002) 339–346.

[4] Z. Djurić, Mechanisms of noise sources in microelectromechanical systems, Microelectronic Reliability 40 (2000) 919–932.

[5] G. Pang, H. Liu, Evaluation of a low-cost MEMS accelerometer for distance measurement, Journal of Intelligent and Robotic Systems 30 (2001) 249–265.

[6] R. Ball, C.P. Lewis, The effect of noise when deriving signals from accelerometers, Measurement and Control 15 (1982) 59–61.

[7] T.L. Paez, B.W. Gibson, Random vibrations measurements with isolated accelerometers, in: Proceedings—Institute of Environmental Sciences, 1992, pp. 95–104.

[8] Y.K. Thong, M.S. Woolfson, J.A. Crowe, B.R. Hayes-Gill, R.E. Challis, Dependence of inertial measurements of distance on accelerometer noise, Measurement Science & Technology 13 (2002) 1163–1172.

[9] Analog Devices webpage: <http://www.analog.com>.

[10] Crossbow webpage: <http://www.xbow.com>.

[11] D.S.G. Pollock, Handbook of Time Series Analysis, Signal Processing and Dynamics, Academic, London, 1999.

[12] J.A. Farrell, M. Borth, The Global Positioning System and Inertial Navigation, Mc Graw-Hill, New York, 1999, p. 91.

[13] Y.K. Thong, A novel computer interface tool using low cost inertial sensors, Ph.D. thesis, University of Nottingham, 2002.

[14] W. Hernández, Improving the response of an accelerometer by using optimal filtering, Sensors and Actuators A: Physical 88 (2001) 198–208.

[15] W. Hernández, Improving the responses of several accelerometers used in a car under performance tests by using Kalman filtering, Sensors 1 (2001) 38–52.